

THEORY OF CRYSTAL STRUCTURES

Investigation of the Properties of Weakly Reflective Metamaterials with Compensated Chirality

I. V. Semchenko^a, S. A. Khakhomov^a, V. S. Asadchy^a, E. V. Naumova^b, V. Ya. Prinz^b,
S. V. Golod^b, A. G. Milekhin^b, A. M. Goncharenko^c, and G. V. Sinitsyn^b

^a *Francisk Skorina Gomel State University, ul. Sovetskaya 104, Gomel, 246019 Belarus*
e-mail: isemchenko@gsu.by; khakh@gsu.by

^b *Institute of Semiconductor Physics, Siberian Branch, Russian Academy of Sciences,
pr. Akademika Lavrent'eva 13, Novosibirsk, 630090 Russia*
e-mail: a_naumova@isp.nsc.ru

^c *Stepanov Institute of Physics, National Academy of Sciences of Belarus,
pr. Nezavisimosti 68, Minsk, 220072 Belarus*
e-mail: g.sinitsyn@ifanbel.bas-net.by

Received July 1, 2013

Abstract—The properties of an artificial anisotropic structure formed by microhelices have been numerically simulated by the example of a specially designed sample. The sample contains paired helices with right- and left-handed twisting directions, due to which the metamaterial chirality is compensated for. Helices are characterized by precalculated optimal parameters; as a result, the permittivity and permeability of metamaterial are approximately equal. Therefore, the wave impedance of the structure is close to the impedance of free space in the frequency range near 2 THz and the reflection of normally incident electromagnetic waves is weak. A boundary problem is solved and an analytical expression is obtained for the reflection and transmission coefficients of an electromagnetic wave passing through the structure. The simulated properties of the structure are compared with experimental results.

DOI: 10.1134/S1063774514040178

INTRODUCTION

Artificial composites having chiral properties in the microwave range have been intensively investigated in the last 20 years [1–11]. These studies were mainly motivated by the suggestion that reflectionless coatings of metal surfaces can be developed based on artificial chiral materials. The results of studying artificial chiral materials, aimed at reducing the reflection of electromagnetic waves, were reported in [4–7]. However, it was concluded in [5, 9] that chirality is not of key importance in the formation of reflectionless coatings, and the intensity of reflected electromagnetic waves at a certain frequency can be significantly decreased using nonchiral absorbing layers. Bohren et al. [9] arrived at the same conclusion based on a calculation of the scattering of electromagnetic waves from metal helices in a dielectric medium.

One of the ways to fabricate metamaterials is the simultaneous use of straight-line and ring conductors as their elements. These elements should satisfy the condition of frequency resonance with the electromagnetic wave used and thus yield the simultaneous manifestation of dielectric and magnetic properties of artificial structure. Another way to fabricate metamaterials, which is proposed here, is based on the use of paired helical elements, which combine dielectric and magnetic properties with simultaneous compensation

for chirality. The absence of chiral properties is due to the fact that each pair consists of right- and left-hand twisted helices. A metamaterial with optimally shaped helical conductors may exhibit equally significant dielectric and magnetic properties at the resonant frequency. This behavior is exotic when compared with the properties of known natural materials and calls for a special analysis in view of further practical application. One advantage of helical elements is the possibility of their activation by both electric and magnetic fields of incident wave, i.e., the possibility of implementing a resonance for different wave polarizations.

Anisotropic and chiral (mirror-asymmetric) properties are characteristic of the most diverse materials and media of natural and artificial origin: crystals, composite structures, and metamaterials [10–18].

The unusual properties of metamaterials have been experimentally studied mainly in the MHz and GHz ranges, where the resonant elements of metamaterial should have millimeter and centimeter sizes; in this case, three-dimensional elements can easily be formed and combined into three-dimensional arrays. Currently, in view of the active development of THz technologies, there is a tendency to design and study metamaterials for the THz range. The set of electromagnetic properties of existing materials in this range is highly limited. For example, there are no materials

with good nonlinear, chiral, or other properties that are widely used in the optical range. Therefore, the concept of metamaterials is very popular in the THz range.

The characteristic sizes of artificial resonant elements for metamaterials of the THz range should lie in the range from several micrometers to several tens of micrometers (i.e., be much smaller than the electromagnetic radiation wavelength). To obtain a matched response, all resonators of a very large array must be tuned with high precision. Among the widely used techniques, only conventional planar technology (which allows one to form planar elements and their layers) provides the desired element sizes with the necessary accuracy. However, the properties of a metamaterial composed of planar elements in principle cannot be set in three dimensions. In addition, researchers have to restrict themselves to one layer of elements (i.e., a metamaterial monolayer) in most experiments because of the limitations imposed by planar technology; this circumstance hinders the analysis of volume electromagnetic properties. At the same time, almost all applications of metamaterials calls for bulky samples with specified three-dimensional electromagnetic properties.

The novelty and scientific importance of the design of metamaterials from three-dimensional shells formed from strained nanofilms [19–22] is in the transition from two-dimensional resonant elements to three-dimensional ones, the precise setting of resonator sizes in the range from micrometers to nanometers (i.e., to the atomic level), and the variety of possible shapes and types of materials used (insulators, metals, or semiconductors). The principle of formation of a shell from a strained film is shown in Fig. 1.

Using three-dimensional designs of resonant shells, one can set an electromagnetic response in three dimensions. This is a new step in the field of designing metamaterials for the THz range which makes it possible to form materials with radically new properties. Currently, this is the only nanotechnology that can offer the mass production of THz metamaterials based on smooth three-dimensional resonant helices, including bulk metamaterials.

OPTIMAL HELIX SHAPE: EQUALITY OF DIELECTRIC, MAGNETIC, AND CHIRAL POLARIZABILITIES

Analytical relations between the dielectric, magnetic, and chiral (magnetoelectric) polarizabilities of small metal helices were derived in [21–23]. It was shown that there is an “optimal” ratio between the helix radius and pitch at which all three polarizabilities are equal at a certain frequency (this ratio was introduced for the helices used as polarization converters).

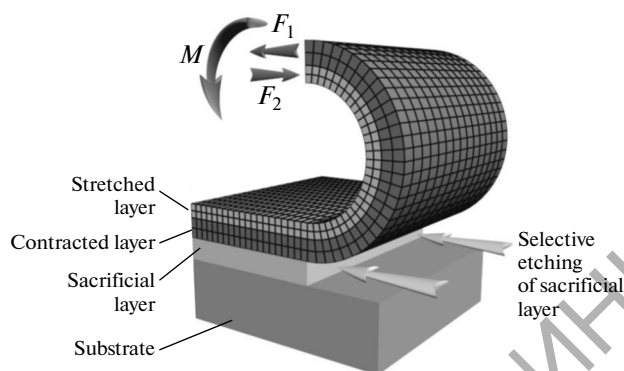


Fig. 1. Schematic diagram of roll-up of a two-layer strained film. A strained film is detached from a substrate by the selective etching of a special (sacrificial) layer. The film detached from the substrate is rolled up under the moment M , caused by internal stress in stretched and contracted layers.

OPTIMIZATION OF THE ARRANGEMENT OF HELICES IN ARRAY

Here we consider the optimization of the arrangement of helices (including paired helices with opposite twisting directions) into an array in order to obtain specific parameters.

A sample with weak reflective properties, composed of one-turn helices with a helix angle of 13.5° , should contain identical numbers of right- and left-handed helices located in the sample plane in both vertical and horizontal directions. The numbers of vertically and horizontally oriented helices should be the same to provide isotropic electromagnetic properties in the sample plane.

To overcome the technological difficulties in preparing a sample containing simultaneously right- and left-handed helices, one can fabricate two samples, one of which consists of only right-handed (vertical and horizontal) helices and the other is composed of only left-handed helices. The desired sample (packet) can be obtained by imposing the former sample on the latter. The second way is to fabricate a sample based on paired helices oriented vertically and horizontally in the sample plane.

The properties of samples of two-dimensional arrays of paired helices were modeled and calculated. The arrays exhibit equally significant dielectric and magnetic properties as a result of using helices with the optimal shape. At the same time, the chiral properties of artificial structures are compensated for, because pairs of optimal helices with right- and left-handed twisting directions are used. As a result, the THz wave impedance of the metamaterial formed is similar to the free-space impedance. The ANSYS HFSS software package was used to analyze the necessary mutual arrangement and orientation of paired helices, which compensate for chirality. Two different ways to arrange paired helices were considered (Fig. 2). In this

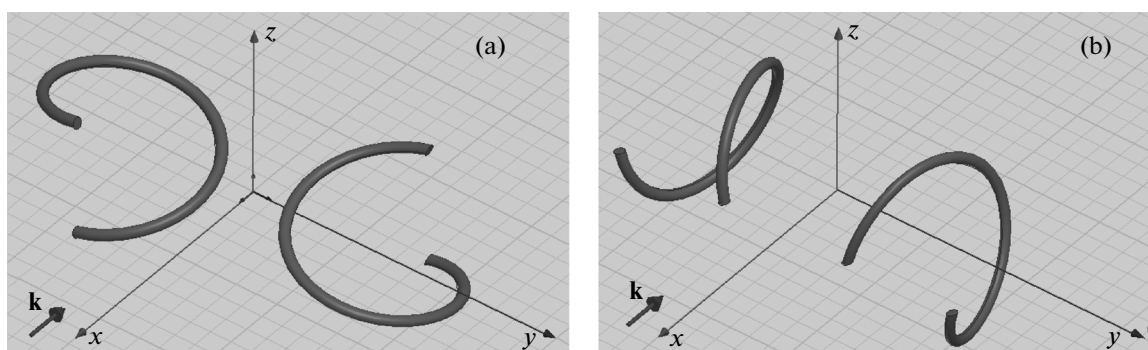


Fig. 2. Versions of mutual arrangement of paired helices aimed at compensating for chirality: (a) right- and left-handed helices have parallel axes and (b) right- and left-handed helices are located on the same axis.

study we located paired helices on one axis (Fig. 2b). As the simulation showed, the sample properties are deteriorated if the helix axes are parallel in each pair (Fig. 2a).

ESTIMATION OF THE EFFECT OF FRAMEWORK SEMICONDUCTOR CYLINDER AND CAPACITANCE OF THE GAP BETWEEN THE ENDS OF RIGHT- AND LEFT-HANDED HELICES

Due to the specific features of the technology of two-dimensional arrays of paired (right- and left-handed) metal helices with an optimal helix angle $\alpha = 13.5^\circ$, the helices must possess cylindrical frameworks made of strained semiconductor films (Fig. 3). The volume of the lateral wall of these cylindrical elements and their concentration were calculated.

It is necessary to estimate the contribution of the semiconductor cylinders forming the framework of helices to the sample permittivity. This contribution should be negligible in comparison with the permittivity of the array of helices. In the opposite case the condition

$$\varepsilon_{eff} = \mu_{eff} \quad (1)$$

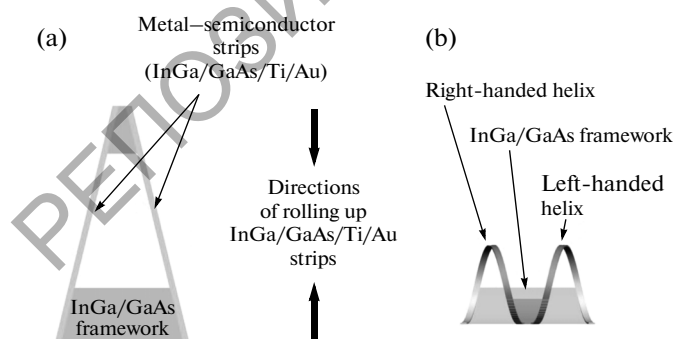


Fig. 3. (a) Initial flat film element and (b) a rolled-up shell (top view).

for the effective permittivity and permeability of the sample will be violated.

This condition yields the proximity of the sample wave impedance to that of free space; i.e., it guarantees the reflectionless properties of the sample in the frequency range under consideration. The validity of condition (1) is provided by the previously calculated optimal parameters of helices, in which an incident wave induces simultaneously electric dipole and magnetic moments. The presence of cylinders (used as helix frameworks) should not lead to a larger reflection coefficient of waves from the artificial structure, i.e., should not violate condition (1). The cylinders used do not have magnetic properties; therefore, they are expected to only slightly affect the effective permittivity of the sample.

The length of each strip for preparing an array of paired helices is approximately equal to half of the electromagnetic field wavelength; in other words, the fundamental-resonance condition is satisfied. If two metal strips are connected into one, the thus formed strip becomes twice as long. Therefore, the resonant frequency of the electromagnetic field decreases by half and the parameters of the helices formed are not optimal. Thus, the initial strips must be disconnected, after which the minimum allowable gap between the strips must be estimated.

The influence of the semiconductor cylinder, which plays the role of a mechanical framework for helices, on the sample properties was studied. It was shown that the contribution of cylinders to the permittivity is small with respect to the contribution of helices. The influence of the dielectric strip that was used to pin helices on the substrate in a specified position (Fig. 4) on the sample permittivity was estimated. It was concluded that the contribution of the dielectric strip, depending on its sizes, is smaller than the contribution of semiconductor cylinder by a factor of 3.9–13.3, i.e., much smaller than the contribution of helices to the sample permittivity.

The capacitance of the gap between the initial film strips (applied to form paired helices) was calculated.

It was shown that, at a gap width of 1 μm, the value used in the experiment (Fig. 4), the helix capacitance plays a much more important role than the gap capacitance.

DETERMINATION OF THE ARRAY PARAMETERS BASED ON THE ANALYSIS OF REFLECTED AND TRANSMITTED WAVES

The following universal relation is satisfied for optimal helices [23–28]:

$$m_x = -\frac{j\omega r^2 q}{2} p_x, \quad (2)$$

where x is the direction along the helix axis, r is the helix radius, $|q| = 2\pi/h$ (h is the helix pitch), ω is the current circular frequency, and j is the imaginary unity. The sign of specific helix twisting q is determined by the twisting helix direction; $q > 0$ for a right-handed helix.

To determine the wave reflection and transmission coefficients, we will consider a sample based on paired helices and solve a boundary problem for a layer, i.e., a structure of finite thickness. Let us introduce the following designations: E^i , E^r , and E^t are, respectively, the incident, reflected, and transmitted waves and L is the effective thickness of the structure.

We assume that the incident wave is linearly polarized and that the vector E^i oscillates along the x axis.

$$E_0^r = \frac{\left(\sqrt{\frac{\varepsilon}{\mu}} - \sqrt{\frac{\mu}{\varepsilon}}\right) (e^{jkL} - e^{-jkL}) E_0^i}{\left(1 - \sqrt{\frac{\mu}{\varepsilon}}\right) \left(1 - \sqrt{\frac{\varepsilon}{\mu}}\right) e^{jkL} + \left(1 + \sqrt{\frac{\mu}{\varepsilon}}\right) \left(1 + \sqrt{\frac{\varepsilon}{\mu}}\right) e^{-jkL}}, \quad (3)$$

where E_0^i is the incident-wave amplitude. Having calculated the squared modulus $|E_0^r|^2$, one can find the reflection coefficient $R = \frac{|E_0^r|^2}{|E_0^i|^2}$. Expression (3) contains the

relation for the wave number $k = \frac{\omega}{c} \sqrt{\varepsilon\mu}$, which is a complex value.

$$E_0^t = \frac{4E_0^i e^{-\frac{j\omega L}{c}}}{\left(1 - \sqrt{\frac{\mu}{\varepsilon}}\right) \left(1 - \sqrt{\frac{\varepsilon}{\mu}}\right) e^{jkL} + \left(1 + \sqrt{\frac{\mu}{\varepsilon}}\right) \left(1 + \sqrt{\frac{\varepsilon}{\mu}}\right) e^{-jkL}}. \quad (5)$$

The wave transmission coefficient can also be found. In a particular case, where relation (4) is valid

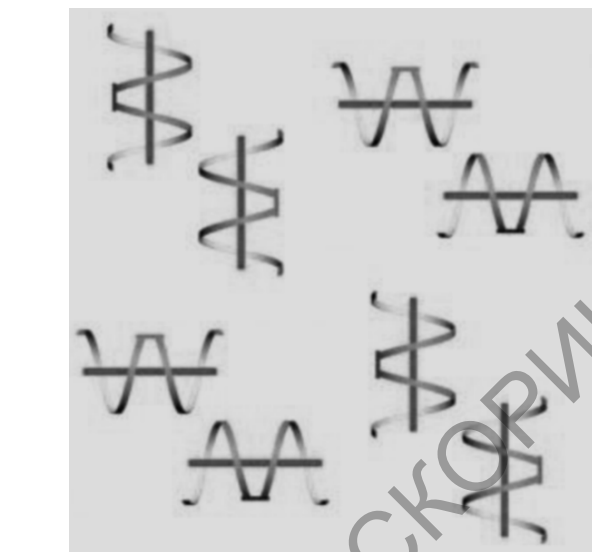


Fig. 4. Schematic diagram of the array of metal–semiconductor helices; straight-line segments indicate dielectric strips fixing helices on the substrate.

Since the sample properties are isotropic in the XOY plane, the generality of the solution to the boundary problem is not violated. Using the condition of continuity of the vectors E and H at the sample boundaries, one can derive the expression for the reflected-wave amplitude:

If the equality

$$\varepsilon = \mu, \quad (4)$$

is satisfied for a critical frequency, according to formula (3), the reflection coefficient becomes zero: $R = 0$.

Let us find the expression for the complex amplitude of the transmitted wave:

at some frequency, the expressions for the transmitted-wave amplitude and the transmission coefficient can

be written as

$$E_0^\tau = \frac{E_0^i e^{-j\frac{\omega}{c}L}}{e^{-j\frac{\omega}{c}(\varepsilon' + j\varepsilon'')L}}, \quad (6)$$

$$T = \frac{|E_0^\tau|^2}{|E_0^i|^2} = e^{-2\frac{\omega}{c}\varepsilon''L}. \quad (7)$$

Here it is taken into account that the metamaterial permittivity is a complex value: $\varepsilon = \varepsilon' + j\varepsilon''$. Having measured the transmission coefficient T for this frequency, one can determine the imaginary part of permittivity (ε'') at this frequency. To this end, one must know the effective thickness of the structure and the critical frequency.

The reflection coefficient R at the critical frequency is zero; in this case, the real part of the permittivity (ε') cannot be measured. To determine ε' , it is necessary to measure the reflection and transmission coefficients, R and T , respectively, at frequencies close to critical.

The solution of the boundary problem described by formulas (3)–(7) turned out to be significantly simplified in view of the following circumstances:

(i) the sample is isotropic in the plane perpendicular to the oz axis, because equal amounts of helices are oriented along the ox and oy axes;

(ii) the artificial structure does not possess chiral properties because it consists of paired helices (i.e., contains identical numbers of right- and left-handed helices);

(iii) the sample exhibits equally significant dielectric and magnetic properties because it consists of helices with optimal parameters.

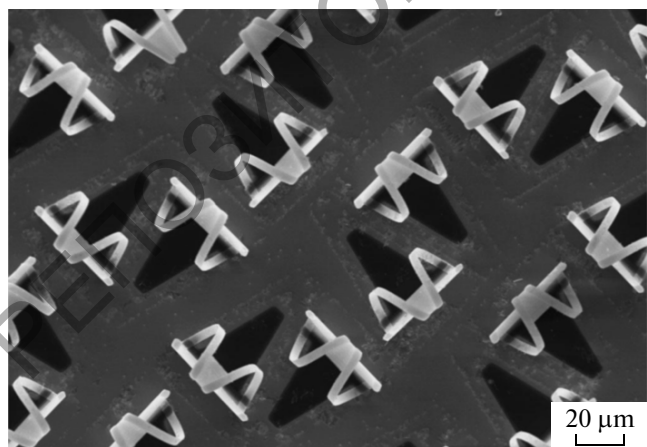


Fig. 5. SEM image of an array of one-turn InGaAs/GaAs/Ti/Au helices.

COMPARISON OF THE EXPERIMENTAL DATA AND RESULTS OF NUMERICAL SIMULATION

The above-described metamaterials based on helices for the THz range can be experimentally implemented using the method of precise 3D nanostructuring developed by Russian researchers [19–22]. Samples in the form of arrays composed of right- and left-handed metal helices on semiconductor frameworks with pairs of helices oriented horizontally and vertically in the sample plane (Fig. 5) have been prepared at the Institute of Semiconductor Physics of the Siberian Branch of the Russian Academy of Sciences (SB RAS). Figure 5 shows a corresponding scanning electron microscopy (SEM) image.

An unfolded strip has a length of 65 μm and a width of 3 μm . The strips are made of an In_{0.2}Ga_{0.8}As/GaAs/Ti/Au (16/40/3/65 nm) film. The helix angle is 13.5° and the radius is 12.4 μm . The concentration of helices in the array is $2.3 \times 10^{13} \text{ m}^{-3}$. The helix angle was chosen to be 13.5°, a value optimal for equal electric and magnetic polarizabilities of helix [23, 24].

The characteristics of the samples were experimentally studied at the Institute of Semiconductor Physics (SB RAS); the results are presented in Fig. 6, which also shows the results of a numerical simulation of the properties of artificial anisotropic structure. The structural parameters for the simulation were chosen to correspond to those of experimental samples: $L = 65 \times 10^{-6} \text{ m}$, $\alpha = 13.5^\circ$, $\omega_0 = 12.6 \times 10^{12} \text{ rad/c}$, $\rho = 2.42 \times 10^{-8} \text{ } \Omega \text{ m}$, and $N_h = 2.3 \times 10^{13} \text{ m}^{-3}$.

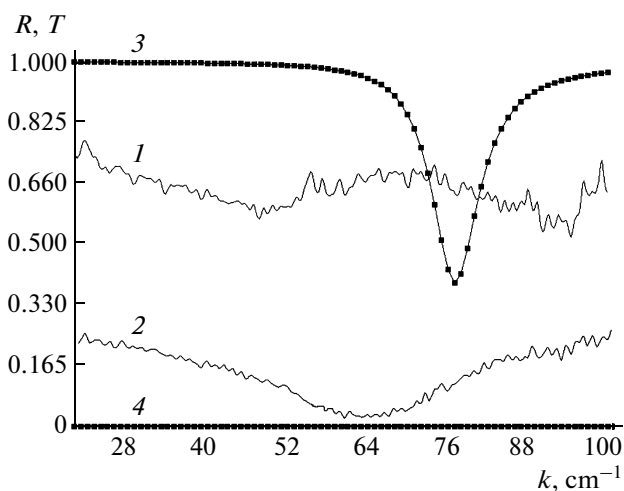


Fig. 6. Dependence of the (1, 3) transmission and (2, 4) reflection coefficients of waves passing through the metamaterial on the wave number: (1, 2) experimental data and (3, 4) simulation results.

CONCLUSIONS

A sample of a weakly reflective metamaterial with compensated chirality was developed based on paired smooth helices with optimal parameters. The metamaterial properties were numerically simulated, and the simulation results were compared with the experimental values of the reflection and transmission coefficients of electromagnetic waves in the THz range.

The metamaterial based on an array of paired helices exhibits equally significant dielectric and magnetic properties, which are due to the optimal shape for helices. The chiral properties of the artificial structure are compensated for because of the use of paired optimal helices with right- and left-twist directions. As a result, the wave impedance of this material in the THz range is close to the free-space impedance.

The influence of the semiconductor cylinder used as a framework for metal helices on the sample properties was investigated. The capacitance of the gap between the initial film strips used to form paired helices was calculated and the gap and helix capacitances were compared.

The boundary problem was solved and necessary calculations were carried out to determine the reflection and transmission coefficients of electromagnetic wave as functions of the sample parameters. The solution to the boundary problem confirmed that the sample exhibits weak reflective properties near the previously determined resonant frequency.

Based on the results, one can develop and fabricate metamaterials composed of optimal helical elements for the THz range. New metamaterials with a negative refractive index can be formed to implement a flat lens for the THz range.

A comparison of the experimental plots and simulation results suggests that the proposed model adequately describes the properties of the artificial structure with compensated chirality. The frequency dependences of the transmission and reflection coefficients, calculated within the proposed model, are in qualitative agreement with the experimental data.

The difference between the experimental data and simulation results is explained by the small thickness of metal layers and their high inhomogeneity, as a result of which some characteristics of helical elements deviated from the calculated ones.

ACKNOWLEDGMENTS

This study was supported by the Belarussian Republican Foundation for Basic Research, project no. F12SO-039, and the Siberian Branch of the Russian Academy of Sciences, integration projects nos. 28 and 128.

REFERENCES

1. A. Priou, A. Sihvola, S. A. Tretyakov, and A. Vinogradov, *Advances in Complex Electromagnetic Materials* (Kluwer, 1997).
2. J. H. Cloete, *Proc. Bianisotropics'97, Univ. of Glasgow, 1997*, p. 39.
3. X. Lafosse, *Proc Chiral-94, Perigueux, France, 1994*, p. 209.
4. K. W. Whites and C. Y. Chang, *J. Electromagn. Waves Appl.* **11**, 371 (1997).
5. S. A. Tretyakov, A. A. Sochava, and C. R. Simovski, *Electromagnetics* **16**, 113 (1996).
6. J. H. Cloete, M. Bingle, and D. B. Davidson, *Proc. Int. Conf. "Electromagnetics in Advanced Applications", Torino, Italy, 1999*, p. 55.
7. S. A. Tretyakov and A. A. Sochava, *Electron. Lett.* **29**, 1048 (1993).
8. I. V. Semchenko, S. A. Khakhomov, S. A. Tretyakov, et al., *J. Phys. D* **31**, 2458 (1998).
9. C. F. Bohren, R. Luebbers, H. S. Langdon, and F. Hunsberger, *Appl. Opt.* **31** (30), 6403 (1992).
10. F. I. Fedorov, *Theory of Girotopy* (Nauka i Tekhnika, Minsk, 1976) [in Russian].
11. B. V. Bokut' and A. N. Serdyukov, *Zh. Eksp. Teor. Fiz.* **6** (5), 1808 (1971).
12. G. S. Landsberg, *Optics* (Nauka, Moscow, 1978) [in Russian].
13. L. D. Landau and E. M. Lifshitz, *Course of Theoretical Physics, Vol. 8: Electrodynamics of Continuous Media*, 3rd ed. (Nauka, Moscow, 1992; Pergamon, New York, 1984).
14. V. M. Agranovich and V. L. Ginzburg, *Crystal Optics with Spatial Dispersion and Excitons*, 2nd ed. (Nauka, Moscow, 1979; Springer, New York, 1984).
15. A. H. Sihvola and I. V. Lindell, *Microwave Opt. Tech. Lett.* **4**, 195 (1991).
16. J. A. Kong, *Electromagnetic Wave Theory* (Wiley, New York, 1986).
17. V. V. Varadan, A. Lakhtakia, and V. K. Varadan, *J. Appl. Phys.* **63**, 280 (1988).
18. V. V. Shevchenko, *Sorosovskii Obrazovat. Zh.*, No. 2, 109 (1998).
19. V. Ya. Prinz, V. A. Seleznev, A. K. Gutakovskiy, et al., *Physica E* **6**, 828 (2000).
20. E. V. Naumova and V. Ya. Prints, Patent RF No. 2317942, 2008.
21. E. V. Naumova, V. Ya. Prinz, V. A. Seleznev, et al., *Proc. Metamaterials, Rome, Italy, 2007*, p. 74.
22. E. V. Naumova, V. Ya. Prinz, S. V. Golod, et al., *Optoelectron., Instrumentation, Data Processing* **45** (4), 292 (2009).
23. I. V. Semchenko, S. A. Khakhomov, and A. L. Samofalov, *Izv. Vyssh. Uchebn. Zaved., Fiz.* **52** (5), 30 (2009).
24. I. V. Semchenko, S. A. Khakhomov, and A. L. Samofalov, *Radiotekh. Elektron.* **52** (8), 917 (2007).
25. I. V. Semchenko, S. A. Khakhomov, and S. A. Tretyakov, *Eur. Phys. J. Appl. Phys.* **46** (3) (2009).
26. I. V. Semchenko, S. A. Khakhomov, and A. L. Samofalov, *Electromagnetics* **26** (3–4), 219 (2006).
27. I. V. Semchenko, S. A. Khakhomov, and E. A. Fedosenko, *Advances in Electromagnetics of Complex Media and Metamaterials, NATO Science Series II, Vol. 89* (Kluwer, Dordrecht, 2003), p. 245.
28. I. V. Semchenko, S. A. Khakhomov, E. V. Naumova, et al., *Crystallogr. Rep.* **56** (3), 366 (2011).

Translated by Yu. Sin'kov